

# Local-game Decomposition for Multiplayer Perimeter-defense Problem

Daigo Shishika and Vijay Kumar

**Abstract**—This paper studies a multi-player game between intruders and defenders. The intruder team tries to score by sending as many intruders as possible to the target. The defender team tries to minimize this score by intercepting the intruders. Finding the strategies for both teams and estimating the outcome of the game is challenging due to the high dimensionality of the joint state space. The state-of-the-art method decomposes the game into two-player games and reduces the design of the defense strategy to an assignment problem, whose solution gives an upper bound on the score. We investigate the cooperative aspects of the multi-player game that are not captured in the aforementioned approach and propose a decomposition method that leads to the formation of local sub-teams. We use the method to design a cooperative-intrusion strategy that guarantees a lower bound on the score. The presented results enable a more accurate estimation of the game outcome, and are expected to be useful in the design and evaluation of defender-team strategies.

## I. INTRODUCTION

Pursuit-evasion games (PEGs) have been studied for various applications under differing assumptions on the players and the environments. Taxonomy and surveys of the research in the field have been presented, for example, in [1] and [2]. In the past decade, PEGs that involve multiple players have attracted research interests [3]–[6]. However, most of the studies are limited to games played between a team and a single agent.

Problems involving multiple agents on both sides have been explored much less, despite their applicability to many realistic scenarios. The main challenge lies in their complexity with a high dimensional state space, and practical approaches have been studied to make such problems tractable. Pierson et al. [7] proposed a distributed algorithm for a team of agents to pursue multiple evaders using a Voronoi tessellation, where the complexity was reduced by considering the Voronoi neighbors of each player. Chen et al. [8] reduced the complexity by decomposing the game into two-player games and then performing assignments of pursuers to intruders.

This paper considers a variant of PEG called the target-guarding problem, which was first introduced by Isaacs [9]. The evader/intruder tries to reach a target without being captured by the pursuer/defender [10], [11]. The defender’s goal is to either intercept the intruder or delay its intrusion indefinitely. Again, the problem is difficult to solve when there are multiple defenders and intruders. We study a ver-

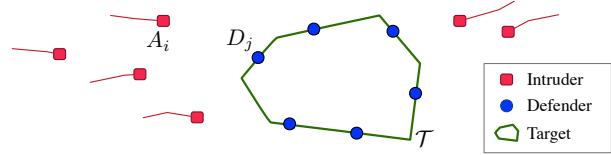


Fig. 1. Illustration of the perimeter-defense scenario.

sion of this problem in the context of defending a perimeter of a region from intruders.

Closely related work by Chen et al. [8], [12] approximated the multi-player game as a combination of two-player games. The solution to the two-player game (strategies and winning regions) was obtained by the differential-game approach [8] and an approximation method termed the “path-defense” approach [12]. These two methods both utilized numerical tools to obtain solutions even in the presence of obstacles and complex game geometries. In contrast, this paper presents a solution that lends itself to a simple geometrical interpretation, by considering the case with no obstacles and assuming that the defenders move on the perimeter.

For the multi-player game, Chen et al. [8], [12] proposed an assignment method; i.e., each defender is assigned to a unique intruder. The assignment determines the behavior of each defender, and also gives an upper bound on the intruder’s score. This paper studies the possibility of a more explicit form of cooperation that cannot be captured by the two-player game, and proposes a decomposition method that reduces the problem to smaller local-games played by subsets of the agents.

The contributions of the paper are (i) the solutions to the two-player game that lends itself to a simple geometric interpretation; (ii) a decomposition method that provides a new way of analyzing the multi-player game; (iii) a team strategy for the intruders that gives a lower bound on the score. We believe these results will be useful for designing and evaluating defender-team strategies in the future.

Section II formulates the perimeter-defense problem. Section III presents the solutions to the two-player game. Section IV discusses how the game changes in the presence of multiple players. Section V proposes the decomposition method and a team strategy for the intruders. Section VI provides simulation results. Section VII concludes the paper.

## II. PROBLEM FORMULATION

Consider two sets of agents:  $\mathbf{A} = \{A_i\}_{i=1}^{N_A}$  denoting  $N_A$  intruders, and  $\mathbf{D} = \{D_i\}_{i=1}^{N_D}$  denoting  $N_D$  defenders. All agents have first-order integrator dynamics on a planar game space  $\Omega$ . Let  $\mathbf{x}_{D_i}$  and  $\mathbf{x}_{A_j}$  denote the position of defender  $i$

We gratefully acknowledge the support of ARL grant ARL DCIST CRA W911NF-17-2-0181

The authors are with the GRASP Lab at the University of Pennsylvania, Philadelphia, USA. {shishika, kumar}@seas.upenn.edu

and intruder  $j$ . We will drop the indices  $i$  and  $j$  when they are irrelevant. The control inputs are the velocities:  $\dot{\mathbf{x}}_D = \mathbf{v}_D$  and  $\dot{\mathbf{x}}_A = \mathbf{v}_A$ , where the magnitudes are constrained by their maximum speeds:  $v_D = \|\mathbf{v}_D\| \leq \bar{v}_D$  and  $v_A = \|\mathbf{v}_A\| \leq \bar{v}_A$ . The ratio of maximum speeds is described by the parameter

$$\nu = \frac{\bar{v}_A}{\bar{v}_D} \in (0, 1].$$

We assume that defenders cannot move inside of the target region  $\mathcal{T}$ . This constraint is motivated, for example, by ground vehicles defending the perimeter of a building. We also assume that the defenders start and move on the perimeter of  $\mathcal{T}$ . Finally, we assume complete knowledge, i.e., all states (positions) are known to all agents, but not the control inputs (velocities).

For two points on  $\mathcal{T}$ , we use  $\text{Arc}(\mathbf{x}_i, \mathbf{x}_j)$  to denote the arc length from  $\mathbf{x}_i$  to  $\mathbf{x}_j$  measured in the counterclockwise direction. Let  $L_c$  denote the circumference of  $\mathcal{T}$ . The opposite point  $\mathbf{x}_{D_i}^{opp}$  is a point such that  $\text{Arc}(\mathbf{x}_{D_i}^{opp}, \mathbf{x}_{D_i}) = L_c/2$ . Finally, we define  $r_i \triangleq \min_{\mathbf{x} \in \mathcal{T}} \|\mathbf{x}_{A_i} - \mathbf{x}\|$  as the distance from intruder  $i$  to the target  $\mathcal{T}$ .

In a microscopic view, each intruder wins/scores if it reaches the target (i.e.,  $r_i(t_s) = 0$ ) without being captured by the defenders (i.e.,  $\|\mathbf{x}_{A_i}(t) - \mathbf{x}_{D_j}(t)\| > 0, \forall D_j \in \mathbf{D}, \forall t < t_s$ ), and a defender wins by intercepting the intruder or preventing it from scoring indefinitely.

In a macroscopic view, victory as a team is defined by the overall points scored by the intruders, which is the main interest of this work: how many intruders can reach the target? We use  $Q_A \in \mathbb{N}$  to denote the score. Given a set of initial conditions, we seek a method to compute bounds on the achievable score.<sup>1</sup>

### III. TWO-PLAYER GAME

This section solves the game between one defender ( $D$ ) and one intruder ( $A$ ), which is the first building block to analyze the overall multi-player game. We first consider the case when  $\mathcal{T}$  is a circular region and then extend the results to general convex shapes.

#### A. Strategies for Circular Target

Without loss of generality, consider  $\mathcal{T}$  to be a unit circle. Symmetry allows us to reduce the state variables to  $\mathbf{z} = [r, \theta]^T$ , where  $r \in \mathbb{R}_{\geq 0}$  is defined earlier (note that polar radius is  $r + 1$ ), and  $\theta \triangleq \theta_A - \theta_D \in (-\pi, \pi]$  is the relative angle wrapped to  $\pi$  (see Fig. 2a). The state vector  $\mathbf{z}$  describes  $\mathbf{x}_A$  measured in the defender frame rotating with  $\theta_D$ .

We parametrize the intruder's control as follows:  $\mathbf{v}_A(v_A, \phi_A) = v_A[\cos(\phi_A), \sin(\phi_A)]^T$ , where  $\phi_A$  is the heading angle in its local frame (see Fig. 2a). The defender's control is the angular velocity:  $\omega_D \triangleq \dot{\theta}_D \in [-\bar{v}_D, \bar{v}_D]$ .

*Lemma 1 (Monotonicity):* Under the optimal strategies on both players,  $|\theta|$  and  $r$  will decrease monotonically until either (i)  $r = 0$  (intrusion); or (ii)  $\theta$  converges to 0.

*Proof:* See Appendix A. ■

<sup>1</sup>Thresholds on the score that defines "victory as a team" are application specific and out of the scope of this work.

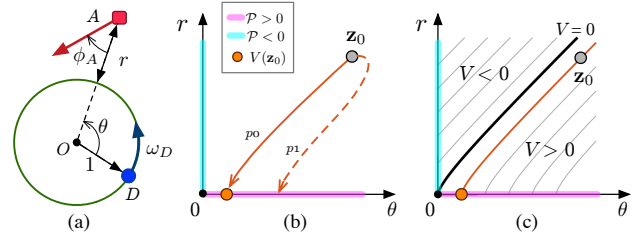


Fig. 2. (a) Definition of the states and control variables for a circular target. (b) Paths of the states in  $r\theta$ -space. Suboptimal defense strategy (path  $p_1$ ) leads to a larger intruder payoff  $\mathcal{P}$  (defined in Appendix). Optimal behaviors by the two players give path  $p_0$ , and the corresponding payoff is  $V(\mathbf{z}_0)$ . (c) Level sets of  $V$  depict the paths of the states under the optimal strategies.

The lemma indicates that  $\theta$  will not change its sign during the game, which simplifies the analysis of the optimal strategies presented next.

*Lemma 2:* The optimal strategies are

$$\omega_D^* = \text{sgn}(\theta)\bar{v}_D, \text{ and} \quad (1)$$

$$v_A^* = \bar{v}_A, \phi_A^* = \text{sgn}(\theta) \sin^{-1}\left(\frac{\nu}{r+1}\right). \quad (2)$$

*Proof:* See Appendix B. ■

The geometric interpretation of these strategies are discussed in Sect. III-B

As a byproduct of the optimal strategies, we obtain the path of the states  $\mathbf{z} = [r, \theta]$  under the optimal strategies on both players. This path is given by the level set of the following function (see Appendix B for the derivation):

$$V = -\sqrt{\left(\frac{r+1}{\nu}\right)^2 - 1} + \cos^{-1}\left(\frac{\nu}{r+1}\right) + |\theta| + c, \quad (3)$$

where  $c = -\cos^{-1}(\nu) + \sqrt{1/\nu^2 - 1}$ . Under the optimal strategies, the states move along the level set of the function  $V = V(\mathbf{z}; \nu)$  until either  $r = 0$  or  $\theta = 0$  occurs.  $V$  is called the Value of the game [9], which is determined by the initial condition  $\mathbf{z}_0 = [r_0, \theta_0]$ . Noting that  $V([0, 0]; \nu) = 0$ , we can conveniently assess whether  $r = 0$  occurs first or  $\theta = 0$  occurs first by looking at the sign of  $V(\mathbf{z}_0)$  (see Fig. 2c). With some abuse of notation, we also write  $V(\mathbf{x}_D, \mathbf{x}_A; \nu)$  to denote  $V(\mathbf{z}; \nu)$ , since  $\mathbf{z}$  is uniquely determined by  $(\mathbf{x}_D, \mathbf{x}_A)$ .

The *winning region* is a concept useful in determining whether a given configuration leads to intrusion or not.

*Lemma 3 (Winning Regions):* For a given  $\mathbf{x}_{D_i}$ , define the *intruder-winning region*  $\mathcal{R}_A(D_i) \triangleq \{\mathbf{x} \mid V(\mathbf{x}_{D_i}, \mathbf{x}; \nu) > 0\}$  and the *defender-winning region*  $\mathcal{R}_D(D_i) \triangleq \Omega \setminus \mathcal{R}_A(D_i)$ . The intruder wins against  $D_i$  if  $\mathbf{x}_A(t_0) \in \mathcal{R}_A(D_i)$  and loses if  $\mathbf{x}_A(t_0) \in \mathcal{R}_D(D_i)$  (see Fig. 3a).

*Proof:* From the initial configuration corresponding to  $V > 0$ , the state  $\mathbf{z}$  reaches the  $\theta$ -axis (see Fig. 2c), meaning that  $r = 0$  occurs first. On the other hand, if  $V < 0$ , the state reaches the  $r$ -axis (i.e.,  $\theta = 0$ ) and stays there. Therefore, the only way for the intruder to enter  $\mathcal{R}_A(D_i)$  is by passing through  $\mathbf{x}_{D_i}$ . Then either of the following holds: (i) the intruder is outside of  $\mathcal{R}_A(D_i)$  indefinitely (it never scores); or (ii) it approaches  $\mathbf{x}_{D_i}$  in finite time (interception). ■

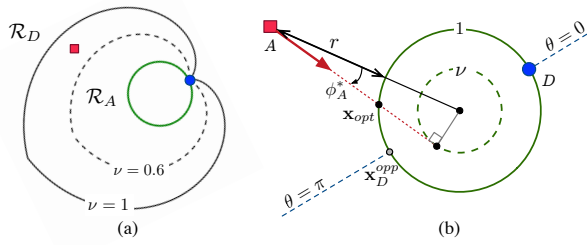


Fig. 3. (a) Boundary of the intruder-winning region given by the level set  $V = 0$  for two values of  $\nu$ . The intruder shown wins if  $\nu = 1$  but loses if  $\nu = 0.6$ . (b) Optimal breaching point  $\mathbf{x}_{opt}$  and heading angle  $\phi_A^*$ . Also see animations at [<https://youtu.be/gR2zWmWwm2c>]

### B. Geometric Interpretation and Generalization

This section provides geometric interpretations of the optimal strategies and their extensions to  $\mathcal{T}$  with arbitrary convex shapes.

For a given defender position, we can draw two lines: (i)  $\theta = 0$  extending from  $\mathbf{x}_D$ , and (ii)  $\theta = \pi$  extending from the opposite point  $\mathbf{x}_D^{opp}$ . We call the the former the *afferent surface* and the latter the *dispersal surface*. The two together are called the *singular surface* because the optimal strategies of the players change discontinuously when the states pass through the surface, which is captured by  $\text{sgn}(\theta)$  in strategies (1) and (2). Since  $|\theta|$  monotonically decreases, the states move away from the dispersal surface ( $|\theta| = \pi$ ),<sup>2</sup> whereas the afferent surface ( $\theta = 0$ ) attracts the state (Lemma 1).

These surfaces divide the game space  $\Omega$  into the *left region*  $\Omega_L$  ( $0 < \theta < \pi$ ) and the *right region*  $\Omega_R$  ( $-\pi < \theta < 0$ ).

**Defender strategy:** The optimal defender strategy is to move counterclockwise if  $\mathbf{x}_A \in \Omega_L$  and clockwise if  $\mathbf{x}_A \in \Omega_R$  at its maximum speed. Under this strategy,  $\mathbf{x}_A$  converges to the afferent surface.

The intrusion strategy also allows a description free from  $\phi_A$  parametrization. Consider the point  $\mathbf{x}_{opt}$  where the tangent line towards a circle with radius  $\nu$  intersects with the perimeter (Fig. 3b). One can see with a simple trigonometry that (2) is equivalent to moving straight towards  $\mathbf{x}_{opt}$ . When  $\nu = 1$ ,  $\mathbf{x}_{opt}$  coincides with the tangent points on  $\mathcal{T}$  that we define next.<sup>3</sup>

From any intruder position, one can draw two tangent lines to  $\mathcal{T}$ . Considering the intruder's motion towards those points, we define the *left tangent point*  $\mathbf{x}_{tan}^L$  to be the one that generates counterclockwise movement, and the other one is the *right tangent point*  $\mathbf{x}_{tan}^R$  (see Fig. 4b).

**Intruder strategy:** The optimal intruder strategy is to move towards  $\mathbf{x}_{opt}$  (optimal breaching point) on a straight line at its maximum speed. When  $\nu = 1$ ,  $\mathbf{x}_{opt} = \mathbf{x}_{tan}^L$  if  $\mathbf{x}_A \in \Omega_L$ , and  $\mathbf{x}_{opt} = \mathbf{x}_{tan}^R$  if  $\mathbf{x}_A \in \Omega_R$ .

**Winning region:** When the agents have equal speed ( $\nu = 1$ ), the level set of  $V$  corresponds to a curve called

<sup>2</sup>This divergence indicates that the agents do not get stuck in a deadlock situation called “perpetuated dilemma” [9].

<sup>3</sup>In the limit  $\nu \rightarrow 0$ ,  $\mathbf{x}_{opt}$  becomes the point on  $\mathcal{T}$  closest from  $\mathbf{x}_A$ . This means that when  $A$  is slow, it should give up on maximizing the separation in  $\theta$  and only focus on minimizing  $\dot{r}$ .

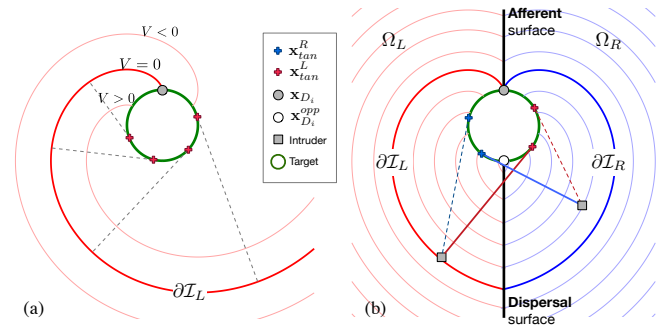


Fig. 4. (a) Left involutes for a circular region. (b) Involute region and singular surfaces. Thin lines are the level sets of  $V$ .

an *involute*. Consider an imaginary taut string wound onto  $\mathcal{T}$ . The involute of  $\mathcal{T}$  is the curve traced out by the tip of the string as it is unwound. Examples are shown in Fig. 4a for a circular region and Fig. 5a for a general convex shape.

There are two ways to wrap (and unwrap) a string. We define the *left involute*  $\partial\mathcal{I}_L(D_i)$  to be the one that leaves  $\mathcal{T}$  from point  $\mathbf{x}_{D_i}$  and is unwound in the counterclockwise direction (red). The *right involute*  $\partial\mathcal{I}_R(D_i)$  is the one unwound in the clockwise direction (blue). Taking the portion of the left and right involutes before they intersect, we can construct a closed curve  $\partial\mathcal{I}(D_i)$ , which turns out to be identical to the level set  $V = 0$ . We define the *involute region*  $\mathcal{I}(D_i)$  to be the region bounded by  $\partial\mathcal{I}(D_i)$ .

Any non-zero  $V$  can be interpreted as the offset in the starting point of the involute, or equivalently, the offset in the length of the string (see Fig 4a). Letting  $\mathbf{x}_A$  denote the tip of the taut string, and  $\mathbf{x}_{opt}$  to be the corresponding tangent point, the following relation holds:

$$V(\mathbf{x}_{D_i}, \mathbf{x}_A; 1) = \text{Arc}(\mathbf{x}_{D_i}, \mathbf{x}_{opt}) - \|\mathbf{x}_A - \mathbf{x}_{opt}\|.$$

Therefore, when  $\nu = 1$ , we can interpret  $V$  as the difference in the time that  $A$  and  $D_i$  arrive at  $\mathbf{x}_{opt}$ . Any positive difference  $V > 0$  indicates that  $A$  arrives at  $\mathbf{x}_{opt}$  first (intruder wins), and negative difference  $V < 0$  means that  $D_i$  can get there first (defender wins).

These offsets generate a family of involutes and enable a construction of the singular surfaces that extends to non-circular  $\mathcal{T}$ .

**Singular surfaces:** Take a pair of left and right involutes with identical offset  $V$ . Note that the two leave  $\mathcal{T}$  from the opposite sides of  $\mathbf{x}_{D_i}$ . Consider the intersection of the two involutes in front of  $\mathbf{x}_{D_i}$ . By continuously varying  $V$  from 0 to  $-\infty$ , the intersection traces out a curve extending from  $\mathbf{x}_{D_i}$  (the afferent surface). Similarly, by varying  $V$  from  $\frac{L_c}{2}$  to  $-\infty$  (where  $L_c$  is the circumference of  $\mathcal{T}$ ), the intersection on the opposite side traces out a curve extending from  $\mathbf{x}_{D_i}^{opp}$  (the dispersal surface). Since these surfaces extend out to infinity, they divide the game space into two regions:  $\Omega_L$  and  $\Omega_R$ .

All the geometries including involutes and singular surfaces can be constructed for  $\mathcal{T}$  with arbitrary convex shapes

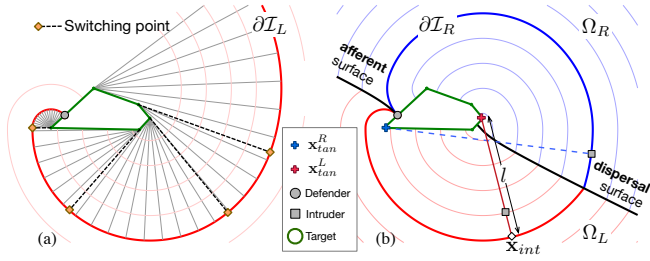


Fig. 5. Involute for a general convex shape. (a) For a polygonal region, curvature as well as the tangent point changes discontinuously at switching points. (b) Optimal strategies apply to general convex shapes when  $\nu = 1$ .

(see Fig. 5). Therefore, we can extend the strategies and winning regions:

**Lemma 4 (Generalization):** When  $\nu = 1$ , the optimal strategies apply to  $\mathcal{T}$  with arbitrary convex shapes, and the boundary of the winning regions is given by the involute  $\partial\mathcal{I}$ .

*Proof:* We prove that (i) the intruder wins if it starts in  $\mathcal{I}$ , and (ii) the defender wins otherwise. Without loss of generality, assume that the intruder starts inside the left region. Consider the line that extends from  $\mathbf{x}_{tan}^L$  through  $\mathbf{x}_A$  and intersects with  $\partial\mathcal{I}_L$  at  $\mathbf{x}_{int}$  (see Fig. 5b). Define the length  $l \triangleq \|\mathbf{x}_{int} - \mathbf{x}_{tan}^L\| = \text{Arc}(\mathbf{x}_{D_i}, \mathbf{x}_{tan}^L)$ . The length  $l$  shrinks at the speed  $\bar{v}_D (= \bar{v}_A)$  when  $D_i$  performs optimally, but not any faster. Therefore, if  $\mathbf{x}_A(t_0) \in \mathcal{I}$ , the intruder can stay in  $\mathcal{I}$  until it reaches  $\mathcal{T}$ . When  $\mathbf{x}_A(t_0) \notin \mathcal{I}$ , the intruder cannot enter  $\mathcal{I}$  from anywhere other than  $\mathbf{x}_{D_i}$ , since the boundary (or  $\mathbf{x}_{int}$ ) moves away at the speed  $\bar{v}_D$ , which the intruder cannot exceed. ■

#### IV. BASIC ANALYSIS OF MULTI-PLAYER GAME

This section discusses how the game changes when there are multiple players. We first review the assignment method proposed by Chen et al. [8] [12]. We then show the benefit of cooperative defense and introduce an extension of the assignment policy. We also present how the optimal intruder strategy changes in the multi-player game.

##### A. Maximum Matching ([8], [12])

For a given initial configuration  $\{\mathbf{x}_{A_i}\}_{i=1}^{N_A}$  and  $\{\mathbf{x}_{D_j}\}_{j=1}^{N_D}$ , the results from Sec. III can be used to determine a set of intruders that each defender can potentially capture<sup>4</sup>: defender  $D_j$  can be assigned to intruder  $A_i$  if  $\mathbf{x}_{A_i} \in \mathcal{R}_D(D_j)$ .

One can generate a bipartite graph with  $\mathbf{A}$  and  $\mathbf{D}$  as two sets of nodes, and the potential assignments defining the edges. Matching in graph theory refers to finding a set of edges so that there is at most one edge extending from each node. In the target-guarding problem, this restriction corresponds to the assumption that  $D_j$  can only play against at most one intruder at a time. Maximum-matching algorithms (see references in [8]) give such an edge set with maximum cardinality.

We say that  $D_j$  is *strongly assigned* to  $A_i$ , if  $D_j$  selects its strategy to be optimal against  $A_i$ . Using the edge set

<sup>4</sup>We loosely use the term “capture” to mean either of the two cases (i.e., no scoring or interception) discussed in the proof of Lemma 3.

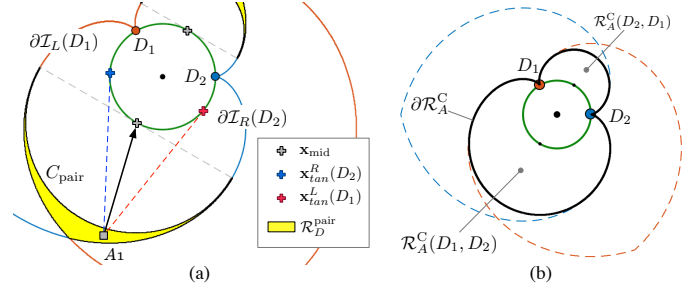


Fig. 6. Two-defenders vs. one-intruder scenario. (a) Additional defender-winning region,  $\mathcal{R}_D^{\text{pair}}$ , enabled by the paired defense. Optimal breaching point for  $A_1$  is now  $\mathbf{x}_{\text{mid}}$ . (b) Intruder-winning region is now  $\mathcal{R}_A^C$ .

given by maximum matching, one can strongly assign a unique intruder to each defender. The assignment gives the guaranteed number of intruders,  $N_A^{\text{cap}}$ , that the defender team can capture. The upper bound on the intruder score is then given by  $Q_A^{\text{upr}} \triangleq N_A - N_A^{\text{cap}}$ .

##### B. Paired Defense

We study how the winning regions and the optimal breaching point change when there are multiple defenders.

Figure 6a depicts the scenario where there are two defenders  $D_1, D_2$  and one intruder  $A_1$ . Since  $\mathbf{x}_{A_1} \in \mathcal{R}_A(D_1) \cap \mathcal{R}_A(D_2)$ , the maximum-matching analysis concludes that no defender can be assigned to  $A_1$ , and thus  $Q_A^{\text{upr}} = 1$ . However, in reality, the optimal breaching point  $\mathbf{x}_{tan}^R(D_1)$  against  $D_1$  is denied by  $D_2$ , and similarly,  $\mathbf{x}_{tan}^R(D_2)$  does not work against  $D_1$ . Now  $A_1$  has to change its strategy.

**Definition 1:** Consider a half-circle region  $C_{\text{pair}}$  with radius  $\rho_c = \text{Arc}(D_1, D_2)/2$  centered at  $\mathbf{x}_{\text{mid}}$  (see Fig. 6a). Construct a curve  $\partial\mathcal{R}_A^C$  by combining  $\partial\mathcal{I}_L(D_1)$ ,  $\partial C_{\text{pair}}$ , and  $\partial\mathcal{I}_R(D_2)$ . The **paired intruder-winning region**<sup>5</sup>,  $\mathcal{R}_A^C(D_1, D_2)$ , is the region bounded by  $\partial\mathcal{R}_A^C$  (see Fig. 6b). Note, there is always another region on the opposite side denoted by  $\mathcal{R}_A^C(D_2, D_1)$  (the arguments are flipped). Also note that the concepts apply to general convex shapes.

**Lemma 5:** The intruder-winning region against a pair of defenders  $D_1$  and  $D_2$  is

$$\mathcal{R}_A^C(D_1, D_2) \cup \mathcal{R}_A^C(D_2, D_1).$$

*Proof:* Assume  $D_1$  and  $D_2$  are both strongly assigned to  $A_1$ . Consider the intrusion strategy:  $\mathbf{x}_{opt} = \mathbf{x}_{\text{mid}}$  (move towards the midpoint). If  $\mathbf{x}_A \notin \mathcal{R}_A^C$ , then it cannot enter  $\mathcal{R}_A^C$  because the radius  $\rho_c$  is shrinking at the speed  $\bar{v}_D$ . In fact, the distance to  $C_{\text{pair}}$  defined as  $d(t) \triangleq \|\mathbf{x}_{A_1}(t) - \mathbf{x}_{\text{mid}}\| - \rho_c(t)$  does not decrease. Therefore, either  $\mathbf{x}_{A_1} \in \mathcal{R}_D(D_1)$  or  $\mathbf{x}_{A_1} \in \mathcal{R}_D(D_2)$  occurs before  $D_1$  and  $D_2$  meet at  $\mathbf{x}_{\text{mid}}$ . On the other hand, if  $\mathbf{x}_A \in \mathcal{R}_A^C$ , then  $d(t) < 0$  and so  $A_1$  can reach  $\mathbf{x}_{\text{mid}}$  before either  $D_1$  or  $D_2$  does. ■

$\mathcal{R}_D^{\text{pair}}$  in Fig. 6a depicts the regions that are converted from intruder-winning to defender-winning through this paired defense. From the defenders’ perspective, the increase in the

<sup>5</sup>the word “paired” refers to the pairing among the defenders, but not between intruders and defenders.

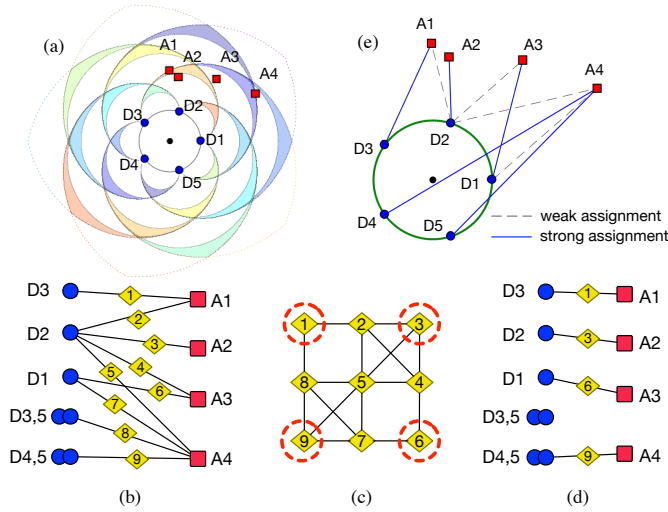


Fig. 7. (a) Example with 5 defenders and 4 intruders. (b) Each node on the left represents a defender or a pair of defenders, and nodes on the right represent intruders. Edges are drawn when the defender or defender pair can win against the intruder. (c) Edges in (b) become nodes in the new graph. A maximum independent set is highlighted in red. (d) An assignment (not necessarily unique) that defends against maximum number of intruders. (e) Assignment described in the original game space.

defender-winning region by  $\mathcal{R}_D^{\text{pair}}$  leads to an extension of the assignment policy presented next.

### C. Maximum Independent Set (MIS) Formulation

Now we allow a defender pair to be assigned to a single intruder. Let  $D_{(i,j)}$  denote a pair  $\{D_i, D_j\}$ . The maximum-matching assignment needs to be modified to avoid the conflict where  $D_i$  and a pair  $D_{(i,j)}$  are assigned to distinct intruders, because  $D_i$  cannot pursue two intruders at the same time. We pose the assignment problem into a maximum independent set (MIS) problem [13] as described in the following:

- 1) Construct a bipartite graph with two sets of nodes  $\mathcal{V}_D = \mathbf{D} \cup \{D_{(i,j)}\}_{i,j \in N_D}$  and  $\mathcal{V}_A = \mathbf{A}$ . Each defender pair is also treated as a single node in the set  $\mathcal{V}_D$ .
- 2) For each  $D_i$ , draw edges to all intruders,  $A_k$ , such that  $\mathbf{x}_{A_k} \in \mathcal{R}_D(D_i)$ .
- 3) For each pair  $D_{(i,j)}$ , draw edges to all  $A_k$  such that  $\mathbf{x}_{A_k} \in \mathcal{R}_D^{\text{pair}}$  (see Fig. 6a). Note that intruders independently capturable by either  $D_i$  or  $D_j$  are excluded.

Figure 7a depicts a particular initial condition, and Fig. 7b shows the bipartite graph (nodes with no edges are omitted).

- 4) The edges in the graph are enumerated and become the nodes in the new graph representation (see Fig. 7c).
- 5) Draw an edge between two nodes (in the new graph) whenever they share the same defender or intruder.
- 6) Find MIS, i.e., the largest subset of nodes with no direct connection.

Figures 7d-e illustrate the resultant strong assignments that give  $N_A^{\text{cap}} = 4$  and  $Q_A^{\text{upr}} = N_A - N_A^{\text{cap}} = 0$ . Note that the maximum-matching assignment only guarantees  $N_A^{\text{cap}} = 3$  (giving  $Q_A^{\text{upr}} = 1$ ). For any initial configuration, the MIS

formulation gives equal or tighter upper bound because it considers paired defense in addition to all individual defense.

The downside of the above formulation is the fact that MIS cannot be found efficiently [13]. This drawback motivates us to tackle the multi-player problem without resorting to explicit defender-intruder assignments, as presented in Sec. V.

### D. Numerical Advantage

This section discusses the case when there are more intruders than defenders. A naive lower bound on the score  $Q_A$  is given by the following lemma.

*Lemma 6 (Naive lower bound):* If there are more intruders than defenders, i.e.,  $N_A - N_D = q > 0$ , at least  $q$  intruders reach the target, i.e.,  $Q_A^{\text{low}} = q$ .

*Proof:* If the intruders synchronize their arrival times so that they approach  $N_A$  distinct breaching points all simultaneously, at most  $N_D$  of them can be captured. ■

Despite its simplicity, the above lemma gives an intuition for the intrusion strategy as a team – they should generate a numerical advantage. Depending on the initial positions, a local advantage in the number of agents can occur even when the intruders are outnumbered as a whole ( $N_A \leq N_D$ ).

The above lemma suggests that it may be useful for some intruders to slow down and wait for their teammates that are farther away. This coordination prevents multiple intruders being captured by a single defender (a scenario studied in [14] using a vehicle-routing formulation). However, waiting for a teammate that is too far away may also reduce the score. We build a systematic way to analyze this tradeoff next.

## V. DECOMPOSITION METHOD

This section proposes an approach to analyze the multi-player game without performing one-to-one assignment between the defenders and intruders. The proposed decomposition method is used to construct a team strategy for the intruders that guarantees a lower bound on their score.

### A. Local-game Regions & Defender Sub-teams

We unify the attacker-winning regions from the individual defense (two-player game) and from the paired defense as follows:

*Definition 2:* The **local-game region** (LGR) generated by an ordered pair  $(D_i, D_j)$  is

$$\mathcal{R}_{\text{LG}}(i, j) \triangleq \begin{cases} \mathcal{R}_A^C(D_i, D_j) & i \neq j \\ \mathcal{R}_A(D_i) & i = j \end{cases}, \quad (4)$$

where  $\mathcal{R}_A^C$  is defined in Def. 1. We refer to the ordered pair as the *boundary defenders*,  $\mathcal{B} \triangleq (D_i, D_j)$ .

There are two LGRs for every  $\binom{N_D}{2}$  defender pairs (when  $i \neq j$ ), and also  $N_D$  LGRs for the case  $i = j$ . Therefore, the total number of LGRs is  $2 \times \frac{N_D(N_D-1)}{2} + N_D = N_D^2$ , and we use the superscripts  $k \in \{1, \dots, N_D^2\}$  to enumerate the LGRs: e.g., in Fig. 8a,  $\mathcal{R}_{\text{LG}}^6 = \mathcal{R}_A^C(D_3, D_5)$  and  $\mathcal{B}^6 = (D_3, D_5)$ .

*Definition 3:* The **defender sub-team**,  $\mathcal{S}_D^k \subset \mathbf{D}$ , is the subset of defenders that are contained in  $\mathcal{R}_{\text{LG}}^k$ . Note that  $\mathcal{B}^k$

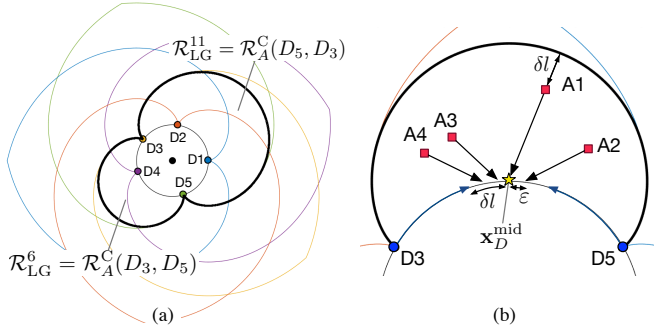


Fig. 8. (a) Example of local-game regions generated by the boundary defenders  $\{D_3, D_5\}$ . Corresponding defender sub-teams are  $\mathcal{S}_D^6 = \{D_4\}$  and  $\mathcal{S}_D^{11} = \{D_1, D_2\}$ . (b) Illustration of intruder's local-game strategy.

are excluded from the subteam (e.g., in Fig. 8a,  $\mathcal{S}_D^6 = \{D_4\}$ ). We use  $n_D^k \triangleq |\mathcal{S}_D^k|$  to denote its cardinality.

A larger LGR (in terms of  $n_D$ ) contains some of the smaller LGRs:  $\mathcal{S}_D^i \subset \mathcal{S}_D^j \Leftrightarrow \mathcal{R}_{LG}^i \subset \mathcal{R}_{LG}^j$ .

### B. Local Intrusion Strategy

The significance of the LGRs is the fact that any intruder in  $\mathcal{R}_{LG}^k$  has a strategy (breaching point) to win against all the defenders in  $\mathbf{D} \setminus \mathcal{S}_D^k$ . By staying in  $\mathcal{R}_{LG}^k$ , the intruders can play a local game that only involves  $\mathcal{S}_D^k$  and no other defenders.

**Lemma 7 (Local-game score):** Consider a subset of intruders  $\mathcal{S}_A \subseteq \mathbf{A}$ , and let  $n_A \triangleq |\mathcal{S}_A|$  be its cardinality. Let  $\mathcal{R}_{LG}^k$  be an LGR that contains all the intruders in  $\mathcal{S}_A$ , i.e.,  $A_i \in \mathcal{S}_A \Rightarrow \mathbf{x}_{A_i} \in \mathcal{R}_{LG}^k$ . If  $q_k \triangleq n_A - n_D^k > 0$ , then the intruder team can score at least  $q_k$  points.

*Proof:* Let  $\mathbf{x}_{\text{mid}}$  denote the optimal breaching point against the defender pair  $\mathcal{B}^k$ . The team strategy we consider is to simultaneously arrive at  $n_A$  distinct points on  $\mathcal{T}$  near  $\mathbf{x}_{\text{mid}}$ , which effectively generates a local  $n_D^k$  vs.  $n_A$  game.

Let  $l$  denote the arc length from the boundary defender to  $\mathbf{x}_{\text{mid}}$  (i.e., the radius of  $C_{\text{pair}}$ ). Let  $A_1 \in \mathcal{S}_A$  denote the intruder farthest from  $\mathbf{x}_{\text{mid}}$ , and define  $\delta l \triangleq l - \|\mathbf{x}_{A_1} - \mathbf{x}_{\text{mid}}\|$  (see Fig. 8b). Intruder  $A_1$  moves straight towards  $\mathbf{x}_{\text{mid}}$ . When  $A_1$  arrives at  $\mathbf{x}_{\text{mid}}$ , there will be a gap of arc length at least  $2\delta l$  between the two defenders  $\mathcal{B}^k$ . All other intruders  $A_i \in \mathcal{S}_A \setminus A_1$  aim at distinct points  $\{\mathbf{x}_i^{\text{opt}}\}$  around  $\mathbf{x}_{\text{mid}}$  with distance  $\varepsilon$  apart from each other, i.e.,  $\min_{i,j \in \mathcal{S}_A} \|\mathbf{x}_i^{\text{opt}} - \mathbf{x}_j^{\text{opt}}\| = \varepsilon$ .

Selecting a sufficiently small  $\varepsilon$  ensures that all intruders can (i) arrive within the gap, and (ii) arrive at their breaching points no later than  $A_1$  reaches  $\mathbf{x}_{\text{mid}}$ . All intruders coordinate with  $A_1$  to simultaneously arrive at  $\mathcal{T}$ . With the same argument used in Lemma 6, the score  $q_k = n_A - n_D^k$  is guaranteed.

The case when  $\mathcal{B}^k$  is a single defender can be treated similarly by considering the involute region. ■

The intruders can partition  $\mathbf{A}$  into disjoint sub-teams and play separate local games. The question is how to perform such partitioning so that the overall score is maximized.

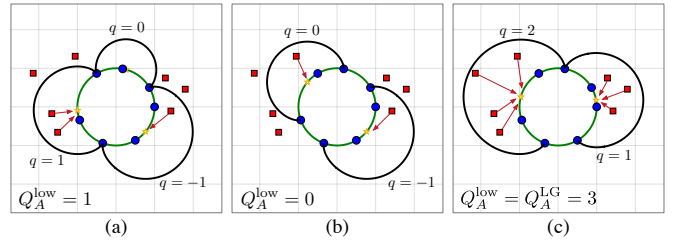


Fig. 9. Computation of  $Q_A^{\text{low}}$  for different choices of  $\mathbf{G}$ . The arrows depict the associated intrusion strategies. The optimal teaming  $\mathbf{G}^*$  is shown in (c).

### C. Sub-team Formation Algorithm

Different grouping of the intruders result in different sets of local-games, local strategies, and the overall score. This section discusses the optimal grouping policy that maximizes the overall intruder score. Since considering all possible grouping called the *set partition problem* is inefficient (NP-complete), we propose a grouping based on LGRs, which leads to a polynomial-time algorithm.

For a given intruder team  $\mathcal{S}_A$ , it is reasonable to assume that they want to play against minimum number of defenders. Therefore, we consider the smallest (in terms of  $n_D$ ) LGR that contains all intruders in  $\mathcal{S}_A$ . Collecting the associated LGRs from all subteams, we define  $\mathbf{G} \subseteq \{1, 2, \dots, N_D^2\}$  to be the set of LGRs that corresponds to the given grouping. The grouping guarantees the following lower bound on the score:

$$Q_A^{\text{low}}(\mathbf{G}) \triangleq \sum_{k \in \mathbf{G}} \max\{q_k, 0\}, \quad (5)$$

where each  $q_k$  is computed based on every subteam-LGR pair (Lemma 7). The following lemma simplifies the search for the optimal teaming:

**Lemma 8 (Disjoint set):** There always exists an optimal grouping  $\mathbf{G}^*$ , which maximizes  $Q_A^{\text{low}}$ , with the following disjointness property:  $\mathcal{R}_{LG}^k \cap \mathcal{R}_{LG}^l = \emptyset$  for  $k, l \in \mathbf{G}^*$ .

*Proof:* Let  $q_1, q_2 > 0$  be the scores of intersecting LGRs in  $\mathbf{G}$ . Consider the smallest LGR that contains the two, whose score is  $q_3$ . We show below that  $q_3 \geq q_1 + q_2$ , indicating that intersecting LGRs can always be replaced by a single LGR without reducing the overall score.

Let  $q_i \triangleq n_A^i - n_D^i$  for  $i = 1, 2$ . Let  $n_D^{\text{int}} \geq 0$  and  $n_A^{\text{add}} \geq 0$  denote the numbers of the defenders in the intersection and intruders in  $\mathcal{R}_{LG}^3 \setminus (\mathcal{R}_{LG}^1 \cup \mathcal{R}_{LG}^2)$ . Then  $q_3 = n_A^1 + n_A^2 + n_A^{\text{add}} - (n_D^1 + n_D^2 - n_D^{\text{int}}) = q_1 + q_2 + n_A^{\text{add}} + n_D^{\text{int}} \geq q_1 + q_2$ . ■

Lemma 8 allows us to reverse the order of selections as follows. Choose a disjoint set of LGRs,  $\mathbf{G}$ . For each  $k \in \mathbf{G}$ , define  $\mathcal{S}_A^k$  to be the set of all intruders in  $\mathcal{R}_{LG}^k$ . We can also associate a unique score  $q_k \triangleq |\mathcal{S}_A^k| - |\mathcal{S}_D^k|$  to each LGR. The computation of  $Q_A^{\text{low}}(\mathbf{G})$  for different choices of  $\mathbf{G}$  is exemplified in Fig. 9. The optimal teaming  $\mathbf{G}^*$  that maximizes (5) gives a total score guaranteed by the intruder team:

$$Q_A^{\text{LG}} \triangleq Q_A^{\text{low}}(\mathbf{G}^*) = \max_{\mathbf{G}} \left( \sum_{k \in \mathbf{G}} \max\{q_k, 0\} \right). \quad (6)$$

It is easy to test whether the intruders can guarantee a score of at least one:  $Q_A^{\text{LG}} > 0 \Leftrightarrow \exists q_k > 0$ .

### Algorithm 1 Intruder Sub-team Formation

```

1:  $\mathbf{A}_{\text{free}} = \{A_1, A_2, \dots, A_{N_A}\}$   $\triangleright$  ungrouped intruders
2: Compute  $q_k, \forall k$ 
3: while  $\mathbf{A}_{\text{free}} \neq \emptyset$  and  $\exists k$  s.t.,  $q_k > 0$  do
4:    $q_M = \max q_k$ 
5:    $\text{cand} = \{j \mid q_j = q_M, j \in \{1, \dots, N_D^2\}\}$ 
6:    $\text{best} = \arg \min_{k \in \text{cand}} n_D^k$ 
7:    $\mathcal{S}_A^{\text{best}} = \{\text{all intruders in } \mathcal{R}_{\text{LG}}^{\text{best}}\}$ 
8:   Append  $\text{best}$  to  $\mathbf{G}$ 
9:    $\mathbf{A}_{\text{free}} = \mathbf{A}_{\text{free}} \setminus \mathcal{S}_A^{\text{best}}$ 
10:  Update  $q_k, \forall k$  with the new  $\mathbf{A}_{\text{free}}$ 
11: end while

```

To calculate the exact score  $Q_A^{\text{LG}}$ , consider a graph with vertices representing the  $N_D^2$  LGRs. Let the local-game score,  $q_k$ , be the weight of the  $k$ 'th vertex. Draw edges between vertices that represent conflicting regions; the edge  $(i, j)$  exists if  $\mathcal{R}_{\text{LG}}^i \cap \mathcal{R}_{\text{LG}}^j \neq \emptyset$ . The optimal teaming and score is obtained from the maximum weight independent set on this graph: the set of vertices whose sum of weights is maximal subject to the constraint that no two vertices are joined by an edge. Fortunately, the graph structure is that of a circular arc graph: each vertex (LGR) can be associated with the perimeter arc between its boundary defenders, and two vertices are in conflict if and only if their arcs intersect. The maximum weight independent set of a circular arc graph with  $n$  vertices can be solved in  $o(n^2)$  time [15]. This provides an  $o(N_D^4)$  complexity algorithm for computing the intruders' guaranteed total score  $Q_A^{\text{LG}}$  and optimal teaming  $\mathbf{G}^*$ .

To solve large problems efficiently we also propose Algorithm 1 (a greedy search). The number of iteration required for Algorithm 1 is bounded by the number of selected sub-teams, which is less than  $N_A$ . Moreover, the first iteration immediately tells us whether  $Q_A^{\text{LG}} > 0$  or  $Q_A^{\text{LG}} = 0$ , which is of interest if  $Q_A = 1$  is the threshold for the intruders' victory. Importantly, this is a question that cannot be answered by maximum-matching or MIS assignment analysis, since they only give upper bounds. Although the grouping from this greedy search may be suboptimal in some cases (discussed in Sec. VI), it always detects a region with  $q_k > 0$  if there exists one.

Finally, another important question is the tightness of  $Q_A^{\text{low}}$  given by the local strategy (Lemma 7) with the optimal teaming  $\mathbf{G}^*$ . The bound is tight if there exists a defender-team strategy that restricts the intruder score to be less than or equal to  $Q_A^{\text{LG}}$ . Designing a team strategy for the defenders that utilizes the decomposition method to achieve the above two conditions is a subject of ongoing work.

## VI. NUMERICAL EXAMPLE

We show an example with  $N_D = N_A = 8$ . In a realistic situation, the intruders and defenders detect each other when they are sufficiently close. To simulate this sensing range, we consider a boundary (the dashed line in Fig. 10b) around the target where the intruders "appear" from the defenders' perspective. We use  $r_s$  to denote the distance of this boundary from  $\mathcal{T}$ .

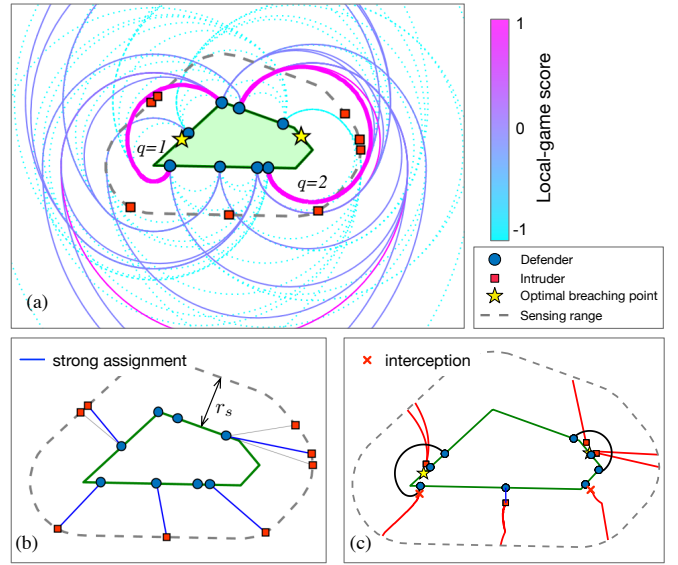


Fig. 10. (a) Boundaries of the local-game regions at the beginning of the game. The colors indicate the local-game scores. (b) Initial defender-intruder assignments (used by the defender team). (c) The snapshot of the game. There are two sub-teams, leading to the overall score  $Q_A = 3$ . Also see animations at [<https://youtu.be/gR2zWmWwm2c>]

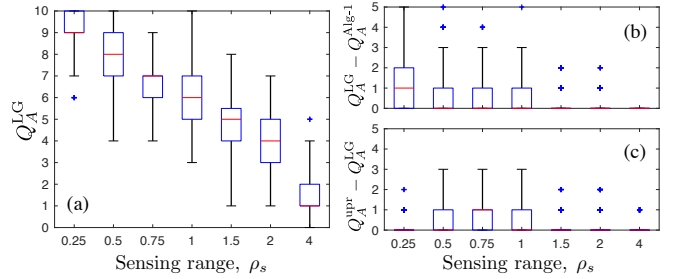


Fig. 11. Statistics from randomly generated initial configurations. (a)  $Q_A^{\text{LG}}$  with varying sensing range  $\rho_s$ . (b) Performance of Algorithm 1 shown by the difference with  $Q_A^{\text{LG}}$ . (c) Tightness of the bounds shown by  $Q_A^{\text{upr}} - Q_A^{\text{low}}$ .

The intruder team uses the local-game decomposition to find the sub-teams and the optimal breaching points. Figure 10a shows the candidate local-game regions (guaranteed scores are indicated by their color). There are two regions selected by Algorithm 1, and the corresponding optimal breaching points are highlighted with stars. The local game on the left gives  $q = 1$ , and the other gives  $q = 2$ , resulting in the lower bound  $Q_A^{\text{low}} = 3$ .

The assignment approach (detailed in Sec. IV) is used for the defending policy. For the given initial configuration, there is no paired defense, so the maximum-matching and MIS assignments give the same result. The upper bound  $Q_A^{\text{upr}} = 3$  is identical to  $Q_A^{\text{low}}$  in this example, indicating that the bounds are tight. Figure 10c shows a snapshot of the simulation.

*Statistical Results:* Since the initial configuration greatly affects the outcome of the game, we obtain the statistics of the score as a function of  $r_s$ . Noting that the average distance between neighboring defenders is  $L_c/N_D$  (which

is proportional to the radius of  $\mathcal{R}_A^C$ ), we use the nondimensionalized quantity  $\rho_s \triangleq r_s N_D / L_c$  to describe the sensing range. Figure 11a shows how  $Q_A^{LG}$  varies with  $\rho_s$ . We used  $N_D = N_A = 10$ , and for each  $\rho_s$ , the statistics are computed from 500 randomly generated initial configurations.

Figure 11b shows the difference between the lower bound computed by Algorithm 1 and the optimal value  $Q_A^{LG}$ . Figure 11c shows the gap between  $Q_A^{upr}$  obtained from the assignment method and  $Q_A^{low}$  obtained from the local-game decomposition method. Finding a team defense strategy to achieve a tighter bound  $Q_A^{upr} = Q_A^{LG}$  is part of ongoing work.

## VII. CONCLUSION

This paper describes an approach to solve the multi-player perimeter-defense problem, which is a game played between intruders and defenders. We derive the solution to the two-player game (1-defender vs. 1-intruder) which lends itself to a simple geometric interpretation and applies to general convex shapes. We discuss additional aspects that emerge in the multiple-player game: (i) change in the individual intrusion strategy, (ii) cooperation among defenders that expands their winning region, and (iii) numerical advantages that lead to a team strategy for the intruders. A decomposition method is proposed to efficiently analyze the overall game, and it is used to design a team strategy for the intruders. The decomposition method as well as the intruder strategy is useful for evaluating and improving team strategies for the defenders.

## APPENDIX

### A. Proof of Lemma 1

Note that  $r = 0$  is necessary for intrusion, and  $\theta = 0$  is necessary for capture. Since the positions are the only states (i.e., first-order dynamics), smaller  $|\theta|$  (resp. larger  $r$ ) is always advantageous for  $D$ . This observation is sufficient to conclude that  $D$  should not increase  $|\theta|$ .

Next, we show that  $D$  can reduce  $|\theta|$  if it uses its maximum speed:  $|\omega_D| = \bar{v}_D$ . Consider the following expression which is well defined everywhere except  $\theta = \{0, \pm\pi\}$ :

$$\frac{d}{dt}|\theta| = \text{sgn}(\theta)\dot{\theta} = -\text{sgn}(\theta)\omega_D \left(1 - \frac{\sin \phi_A v_A}{r+1 \omega_D}\right), \quad (7)$$

If  $|\omega_D| = \bar{v}_D$ , the term inside the parenthesis is bounded as follows:  $1 - \frac{\sin \phi_A v_A}{r+1 \bar{v}_D} \geq 1 - \frac{v_A}{\bar{v}_D} \geq 1 - \nu > 0$ . Therefore, we have  $\frac{d}{dt}|\theta| < 0$  if  $\omega_D = \bar{v}_D \text{sgn}(\theta)$ .

With a similar argument, we can see that  $A$  should always reduce  $r$ , and it is obvious that  $A$  can control the sign of  $\dot{r}$ .

### B. Proof of Lemmas 2

Using the monotonic behavior of  $\theta$  provided by Lemma 1, we can restrict our discussion to the case when  $\theta > 0$ . Since smaller  $\theta$  is always advantageous for  $D$ , we can see that  $D$ 's optimal strategy is to minimize  $\dot{\theta}$ , which is achieved by (1).

The intruder's optimal strategy is more subtle because it can control both  $\dot{r}$  and  $\dot{\theta}$ . Let  $\mathcal{P}$  denote the terminal payoff function that  $D$  minimizes and  $A$  maximizes. For example, it can be  $\mathcal{P} \triangleq \theta(t_f) - r(t_f)$ , where  $t_f$  denotes the time

when the states reach either  $r = 0$  or  $\theta = 0$ . A positive  $\mathcal{P}$  means that  $A$  reached  $\mathcal{T}$  while keeping some distance to  $D$ . A negative  $\mathcal{P}$  means that  $D$  achieved  $\theta = 0$  first.

Consider the trajectory of  $\mathbf{z}$  in the  $r\theta$ -space (see Fig. 2b). Due to the monotonicity, the path of  $\mathbf{z}$  from  $\mathbf{z}(t_0)$  to  $\mathbf{z}(t_f)$  has positive slope everywhere. Let  $\eta$  denote this slope:

$$\eta \triangleq \frac{\dot{r}}{\dot{\theta}} = \frac{v_A \cos \phi_A (r+1)}{\omega_D (r+1 - v_A \sin \phi_A / \omega_D)}. \quad (8)$$

Observe that maximizing  $\eta$  maximizes  $\mathcal{P}$  when starting from the same  $\mathbf{z}(t_0)$ .

By inspection, it is obvious that  $v_A = \bar{v}_A$  maximizes  $\eta$ . Inserting (1) and  $v_A = \bar{v}_A$ , (8) reduces to  $\eta = \frac{\nu \cos \phi_A}{1 - \nu \sin \phi_A / (r+1)}$ . Taking the derivative with respect to  $\phi_A$  and solving  $d\eta/d\phi_A = 0$ , we obtain the optimal heading angle (2). The term  $\text{sgn}(\theta)$  specifies the direction moving away from the defender.

Substituting the optimal strategies into (8) yields the following differential equation:  $d\theta = dr \sqrt{1/\nu^2 - 1}/(r+1)^2$ . By integrating both sides (variables  $\theta$  and  $r$  are separated), we obtain the optimal path (3).

## ACKNOWLEDGMENT

The authors would like to acknowledge valuable discussions with Rattanachai Ramaithitima, James Svacha, Dr. Ani Hsieh, Luis Guerrero, Dr. David Saldaña, Dr. James Paulos, Michael Watterson, Michael Whitzer and Ken Hayashima.

## REFERENCES

- [1] C. Robin and S. Lacroix, "Multi-robot target detection and tracking: taxonomy and survey," *Auton. Robot.*, vol. 40, no. 4, pp. 729–760, 2016.
- [2] T. H. Chung and G. A. Hollinger, "Search and pursuit-evasion in mobile robotics," *Auton. Robot.*, vol. 31, no. 4, pp. 299–316, 2011.
- [3] T. H. Kim and T. Sugie, "Cooperative control for target-capturing task based on a cyclic pursuit strategy," *Automatica*, vol. 43, no. 8, pp. 1426–1431, 2007.
- [4] S. D. Bopardikar, F. Bullo, and J. P. Hespanha, "A cooperative homicidal chauffeur game," *Automatica*, vol. 45, no. 7, pp. 1771–1777, 2009.
- [5] W. L. Scott, "Optimal evasive strategies for groups of interacting agents with motion constraints," Ph.D. dissertation, 2017.
- [6] Z. Zhou, W. Zhang, J. Ding, H. Huang, D. M. Stipanović, and C. J. Tomlin, "Cooperative pursuit with Voronoi partitions," *Automatica*, vol. 72, pp. 64–72, 2016.
- [7] A. Pierson, Z. Wang, and M. Schwager, "Intercepting rogue robots: An algorithm for capturing multiple evaders with multiple pursuers," *IEEE Rob. Autom. Lett.*, vol. 2, no. 2, pp. 530–537, 2017.
- [8] M. Chen, Z. Zhou, and C. J. Tomlin, "Multiplayer reach-avoid games via low dimensional solutions and maximum matching," *Proc. Amer. Control Conf. (ACC)*, pp. 1444–1449, 2014.
- [9] R. Isaacs, *Differential games: A mathematical theory with applications to warfare and pursuit, control and optimization*. Courier Corporation, 1999.
- [10] I. Rusnak, "The lady, the bandits and the body guards - A two team dynamic game". *IFAC Proc.*, vol. 38, no. 1, pp. 441–446, 2005.
- [11] E. Garcia, D. W. Casbeer, K. Pham, and M. Pachter, "Cooperative aircraft defense from an attacking missile," *J. Guid. Control Dyn.*, vol. 38, no. 8, pp. 1510–1520, 2015.
- [12] M. Chen, Z. Zhou, and C. J. Tomlin, "A path defense approach to the multiplayer reach-avoid game," *IEEE Conf. Decision Control (CDC)*, pp. 2420–2426, 2014.
- [13] E. Kleinberg, Jon and Tardos, *Algorithm design*. Pearson, 2006.
- [14] P. Agharkar and F. Bullo, "Vehicle routing algorithms to intercept escaping targets," *Proc. Amer. Control Conf. (ACC)*, pp. 952–957, 2014.
- [15] S. Mandal and M. Pal, "Maximum weight independent set of circular-arc graph and its application," *J. Applied Math. Comput.*, vol. 22, no. 3, pp. 161–174, 2006.